

Publication P8

Sami Ruoho, Jere Kolehmainen, Jouni Ikäheimo, and Antero Arkkio. 2009. Demagnetization testing for a mixed-grade dovetail permanent-magnet machine. IEEE Transactions on Magnetics, volume 45, number 9, pages 3284-3289.

© 2009 Institute of Electrical and Electronics Engineers (IEEE)

Reprinted, with permission, from IEEE.

This material is posted here with permission of the IEEE. Such permission of the IEEE does not in any way imply IEEE endorsement of any of Aalto University's products or services. Internal or personal use of this material is permitted. However, permission to reprint/republish this material for advertising or promotional purposes or for creating new collective works for resale or redistribution must be obtained from the IEEE by writing to pubs-permissions@ieee.org.

By choosing to view this document, you agree to all provisions of the copyright laws protecting it.

Demagnetization Testing for a Mixed-Grade Dovetail Permanent-Magnet Machine

Sami Ruoho^{1,2}, Jere Kolehmainen³, Jouni Ikäheimo³, and Antero Arkkio¹

¹Department of Electrical Engineering, Helsinki University of Technology, FIN-02015 TKK, Finland

²Neorem Magnets Oy, FIN-28400 Ulvila, Finland

³ABB Oy, Motors, Vaasa, Finland

A dovetail machine is a novel design developed to solve the strength problems of traditional buried magnet machines. A mixed-grade construction can be easily applied to a dovetail machine, because a dovetail machine has several magnets in a single pole in different positions. The basic idea of the mixed-grade construction is to use high intrinsic coercivity material in the positions of the high demagnetization risk and high remanence material in the positions of low demagnetization risk. We have developed a demagnetization model that takes into account the temperature dependence of the properties of the permanent-magnet materials to model a dovetail permanent-magnet motor with mixed-grade construction. We compared the model with a real motor. By comparing the testing and the calculations, we show that our demagnetization model can predict the demagnetization of the permanent magnets with reasonable accuracy. We discuss the benefits of the mixed-grade construction in a dovetail machine.

Index Terms—Demagnetization, dovetail machine, finite-element analysis, permanent magnets, synchronous machines.

I. INTRODUCTION

IN a conventional buried-magnet machine, the magnets are assembled in poles in a V-shaped manner, where between the two inclined magnets there is an iron pole. In this construction, there are iron bridges supporting the pole between the magnets. These bridges act as a way for the leakage flux, and thus these bridges are usually kept thin. In a medium- or high-speed machine, the centrifugal forces acting on the poles cause strength problems [1] because of the thin iron bridges (Fig. 1). To solve these problems, a new pole type, named dovetail shaped pole, was developed by Kolehmainen [2]. A dovetail machine and a tradition buried-magnet machine have been compared both electrically and mechanically by Kolehmainen *et al.* [1].

In a dovetail machine, the iron bridges can be kept very thin or the machine can even be built without the iron bridges [3]. This is because the magnets carry the mechanical stresses caused by the centrifugal forces instead of the iron bridges. When compared to conventional designs, dovetail machines with high pole number are mechanically stronger, and with low pole number they are electrically better [4].

The two most important physical properties of a permanent-magnet material are remanence (B_r) and intrinsic coercivity (JH_c). Remanence is related to the ability of the magnet material to produce a magnetic flux. Intrinsic coercivity is related to the ability of the permanent-magnet material to resist irreversible demagnetization, which means losing the ability of flux production. Irreversible demagnetization can be caused by too high temperature or too high magnetic field antiparallel to the magnetization direction or by both. Higher intrinsic coercivity means higher demagnetization resistance of the material.

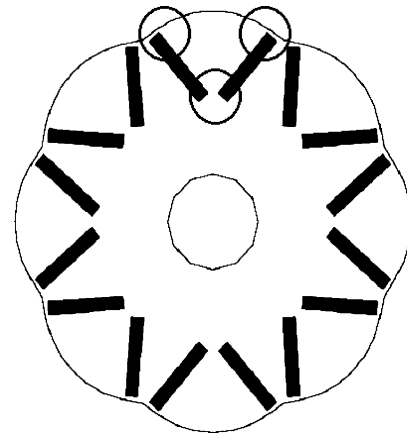


Fig. 1. A conventional buried magnet machine. The iron pole between the magnets is supported by thin iron bridges, which are kept thin because of the leakage flux. The centrifugal forces acting on poles in higher speeds are causing stress on the iron bridges (circled in one pole).

Normally, a machine is built using only one magnet material grade, which is selected as a compromise of a flux production and a demagnetization resistance. When a machine is loaded, different parts of the magnets in a pole can be in different working points and, thus, the same demagnetization resistance is not needed in all magnets. This means that a magnet grade with less intrinsic coercivity and thus higher remanence can be used in the positions, where the high demagnetization resistance is not needed. In a case of Nd-Fe-B magnets, this kind of “mixed-grade pole” construction can produce higher flux while being less expensive than the conventional “single-grade” construction [5]. A dovetail machine is ideal for mixed-grade construction, because in one pole there are three individual magnets circumferentially (Fig. 2).

If a machine is overheated or loaded too heavily, the magnets might get permanently demagnetized. Machines are usually designed so that they are not demagnetized in any realistic fault condition. An irreversible demagnetization of different kind of

Manuscript received January 31, 2009; revised March 17, 2009. Current version published August 19, 2009. Corresponding author: S. Ruoho (e-mail: sami.ruoho@tkk.fi).

Digital Object Identifier 10.1109/TMAG.2009.2019955

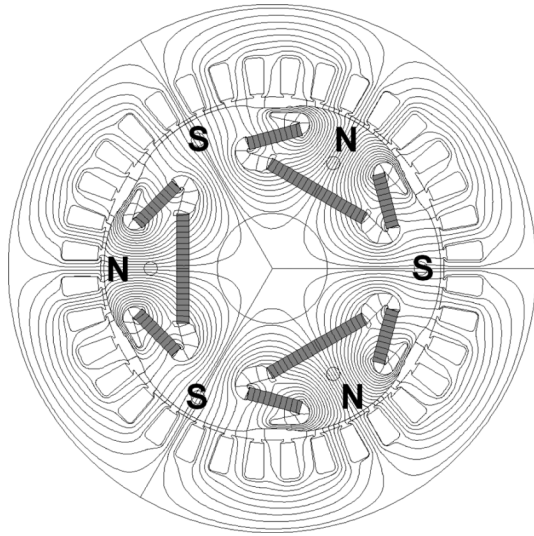


Fig. 2. A cut of the six-pole motor used in these calculations. The rotor is built according to the patented dovetail construction, where the magnets (drawn in dark grey) are utilized to carry the stresses caused by centrifugal forces.

machines is still considered an important research subject, because the phenomenon is studied in several papers. Some authors have used permeance networks [6], while other authors have incorporated their linear demagnetization model in finite-element-method (FEM) analysis tools [7]–[10]. Some authors have used hysteresis models in FEM analysis [11], [12]. In some papers, the demagnetized regions are treated as air assuming total demagnetization [13]. Different demagnetization models have been compared by Ruoho *et al.* [14].

In this paper, a demagnetization resistance of a dovetail machine is studied. The purpose is to compare the results given by calculations with the demagnetization model and the results of the demagnetization testing with the real machine, and to study the suitability of the mixed-grade construction in a dovetail machine.

At first, the demagnetization of the machine is modeled in a locked-rotor situation using a simple demagnetization model taking into account also an inclined field [15]. After that, the machine is tested in an overheated locked-rotor situation while a frequency-converter is feeding an almost sinusoidal current. The demagnetization of the magnets in poles is measured and compared to the results in calculations. Both a single-grade construction and a mixed-grade construction are tested and compared.

II. MOTOR UNDER STUDY

A frequency-converter driven six-pole motor is tested in this research. The basic construction of the rotor is the patented [2] dovetail construction (Fig. 2). The main parameters of the machine can be found in Table I.

Two Nd–Fe–B permanent-magnet material grades are used in a rotor. The second quadrant hysteresis curves of the magnet grades were measured by a hysteresisgraph in 100 °C to define the intrinsic coercivity. The remanence was measured in a room temperature by a Helmholtz coil and an integrator. The demagnetization model [15] needs the values of remanence and intrinsic coercivity in 20 °C and in 150 °C. These values were

TABLE I
MAIN PARAMETERS OF THE MOTOR

Parameter:	Value
Number of poles	6
Outer diameter of the stator	310 mm
Air-gap diameter	165 mm
Core length	165 mm
Number of stator slots	36
Connection	Delta
Input frequency	300 Hz
Rated voltage (phase-to-phase)	370 V
Rated power	45 kW
Maximum power	67 kW

TABLE II
PROPERTIES OF MAGNET MATERIALS

Quantity	Magnet Grade	Value in 20 °C	Value in 150 °C
Remanence	A	1.15 T	0.96 T
Intrinsic coercivity		2440 kA/m	860 kA/m
Remanence	B	1.17 T	0.975 T
Intrinsic coercivity		2210 kA/m	725 kA/m

calculated from the measurements using the temperature coefficients known for the tested materials. The properties of the used magnet grades in 20 °C and in 150 °C can be found in Table II.

Two constructions were tested. In a single-grade construction, all magnets are made of magnet grade A. In a mixed-grade construction, the magnet in the middle of the poles is made of magnet grade B, but the sides of the poles are made of grade A. With this mixed-grade construction, a higher remanence magnet is located in the middle to increase the machine electromotive force (EMF).

During the short-circuit situations, the side magnets are stressed more heavily by a demagnetizing field from the stator than the middle magnets. This is why the middle magnets can be made of a magnet grade with less intrinsic coercivity. Simultaneously, the middle magnets are producing more flux because of higher remanence. The assumption is that the mixed-grade pole made of grades A and B has about the same demagnetization resistance as a single-grade pole made entirely of grade A, while the mixed-grade pole produces more flux. Also, a mixed-grade pole is slightly cheaper, because the grade B has 1 weight-% more neodymium and 1% less dysprosium. In late 2008, the price of Dy was about seven times the price of Nd [16], [17].

III. CALCULATIONS

A locked-rotor situation of the dovetail machine is modeled using a demagnetization model [14], [15] installed in a FEM model developed by Helsinki University of Technology [18]. The hysteresis curves of the magnetic materials are modeled with an exponential model described in [14]. The demagnetization model is adjusted according to the hysteresisgraph measurements to model accurately the magnet grades present. The temperature dependence of the magnetic properties B_r and JH_c is taken into account by a linear interpolation using the values

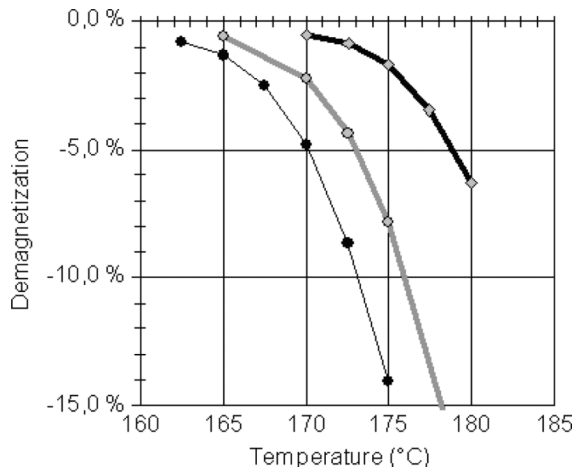


Fig. 3. Calculated demagnetization (drop of EMF) of the motor after a locked-rotor situation with a sinusoidal 100 Hz, 165 A input current as a function of temperature in the locked-rotor situation. Two single-grade constructions (thick black: magnet grade A, thin black: magnet grade B) and one mixed-grade construction (gray) were modeled.

in Table II. In the demagnetization modeling, the inclined demagnetizing field [19] is also considered according to the paper by Ruoho *et al.* [15]. The FEM model used had 3234 quadratic triangular elements and 7377 nodes.

In the calculations, a locked-rotor situation is modeled with a 2-D FEM model. While the rotor is locked, an input current of 165 A and 100 Hz is fed into the stator winding. The calculations have been performed separately for each temperature. The demagnetization of the magnets is calculated both for the single-grade and mixed-grade constructions as a function of temperature. The demagnetization of a whole rotor is modeled by calculating EMF before and after the simulated situation using the 2-D FEM model. The EMF is calculated by setting the input current to 0 A and calculating the voltage.

The calculated demagnetizations as a function of temperature after the locked-rotor situation can be seen in Fig. 3. It can be seen that after the demagnetization is more than 5%, even a small increase of temperature will cause a large increase in demagnetization. Thus, it is important to measure the temperature accurately in testing.

The calculated demagnetization of different magnets in a pole at 175 °C can be seen in Fig. 4. In the single-grade constructions, the side-magnets have the biggest risk of demagnetization. In the mixed-grade construction calculated, the middle-magnet demagnetizes first.

The demagnetization of a single-grade construction made entirely of grade B was modeled in a locked-rotor situation with different currents. The results are presented in Fig. 5. A 10 A change in current will have a change of less than 1% in demagnetization. Thus, the change of current will not have such a drastic impact on the demagnetization as the change of temperature.

For the testing, it was also important to know, if the locking position of the rotor has an effect on the demagnetization of single magnets. For this purpose, a single-grade construction made entirely of grade A was modeled in different locked-rotor

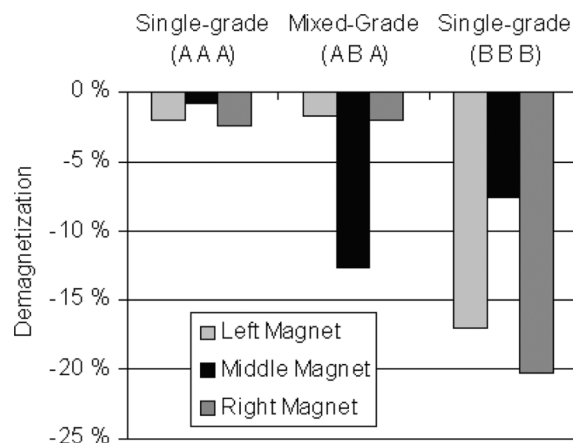


Fig. 4. Calculated demagnetization (drop of magnetization) of the magnets caused by a locked-rotor situation. Two single-grade and one mixed-grade constructions are simulated. Temperature during the situation was 175 °C, a sinusoidal input current of 165 A, 100 Hz was used. The mass of the middle magnet is twice the mass of the side magnet.

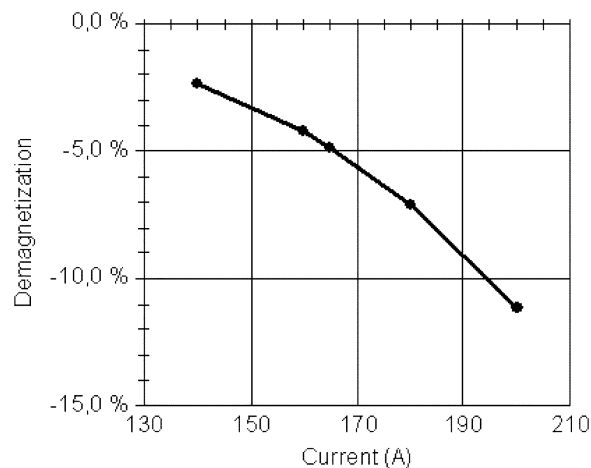


Fig. 5. Calculated demagnetization (drop of EMF) of the motor caused by a locked-rotor situation as a function of the input current amplitude. Temperature was 170 °C. The sinusoidal input current frequency is 100 Hz. It can be seen that the change of the input current by 5 A will cause a change of only 1% in the demagnetization around the point of interest.

positions. The results are presented in Fig. 6. It can be seen that the demagnetization of the right magnet has the strongest dependence on the locking position. This can be a minor problem in testing, because the locking position is not known exactly.

In these calculations, both the drop of EMF and the drop of magnetization are used to measure the demagnetization. The drop of EMF is a very convenient method to model the demagnetization of the whole rotor. The drop of magnetic polarization is practical, when showing a demagnetization of a single magnet.

EMF is modeled in a no-load situation. Only the very thin iron bridges above the magnets are saturated in this situation. Because these bridges are fully saturated, they have a linear behavior, as long as they are kept saturated. Other parts of the motor are not saturated, and thus, practically linear behavior of the magnetic circuit can be expected. This means that the demagnetization calculated from the drop of EMF and from the drop of magnetic polarization are the same.

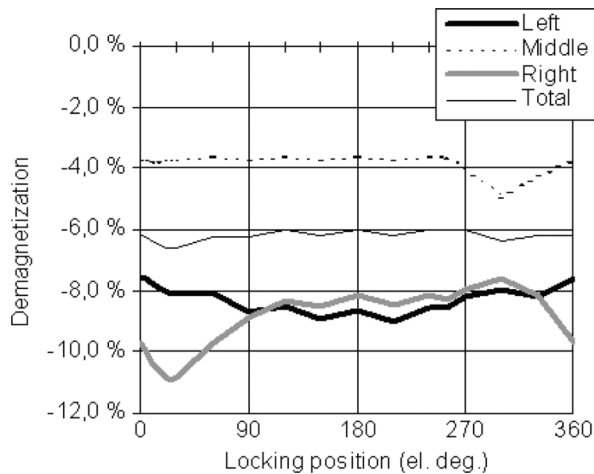


Fig. 6. Calculated demagnetization (drop of EMF) of the side magnets and the middle magnet as a function of the locking rotor position in electrical degrees after 100 Hz, 165 A input current. The rotor is a single-grade construction with grade A only. It can be seen that the demagnetization of the right magnet has the strongest dependence on the locking position.

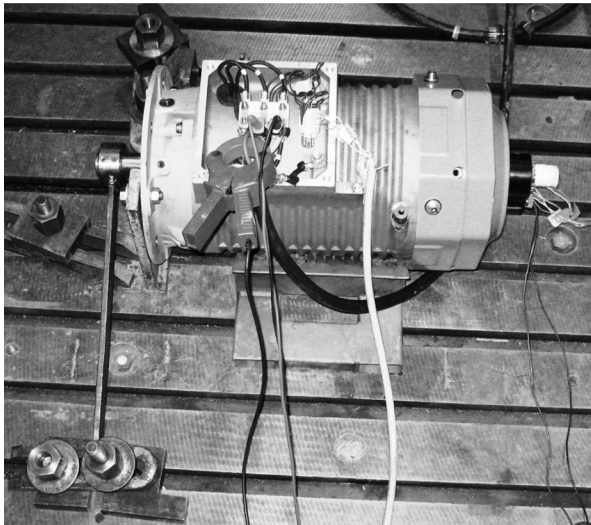


Fig. 7. The test setup. The rotor was locked by the bar on the left during the demagnetization test.

IV. DEMAGNETIZATION TESTING

The results of the calculations were ensured by testing the motor in a real situation. First, the motor was heated up by driving it with one third of the nominal speed while a frequency-converter was feeding a low voltage. The heating of the motor was monitored with seven sensors: three on end-windings and four in the rotor. When the highest temperature reading from the rotor side reached the selected test temperature, the rotor was locked using a steel bar (Fig. 7). After that, a current was fed by a frequency-converter for a couple of seconds.

After the locked-rotor test, the machine was cooled down and the magnets were removed from the rotor. After the removal, the working point of the magnets decreases, because the magnetic circuit has a different permeance when the magnet is in air than when the magnet is inside the rotor. Because the magnets are linear high-coercivity rare-earth magnets, it can be assumed

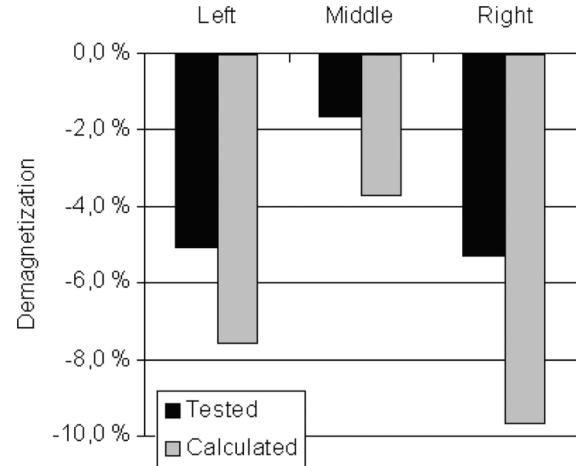


Fig. 8. A measured demagnetization (drop of magnetic polarization) of the poles after the locked-rotor situation with a 100 Hz, 165 A input compared to the calculated demagnetization. This machine had a single-grade construction with grade A only. The mass of the middle magnet is twice the mass of the side magnet.

that the change of working point has a negligible effect on the magnetization.

The remaining total magnetic moment was measured using a Helmholtz coil. After that, the magnets were magnetized to full saturation in a magnetizer. Then, the total magnetic moment was measured again. The ratio of the magnetic moments before and after the saturation was used as a demagnetization of a single magnet.

A single-grade construction using only grade A and a mixed-grade construction using grade B at the middle and grade A on the sides were selected to be tested. The testing scenarios were selected so that the expected total demagnetization would be between -5% and -10% . Because the testing current was around 165 A, the temperature was adjusted according to the results in Fig. 3. The purpose was to test the single-grade construction at 180°C and the mixed-grade construction at 175°C to create the demagnetization of -6.3% and -7.8% , respectively.

V. RESULTS AND DISCUSSION

The tested rotor constructions and the demagnetization test results for the whole rotor are presented in Table III. The demagnetizations are shown magnet by magnet for the single-grade construction in Fig. 8 and for the mixed-grade construction in Fig. 9.

The calculated values and test results show a difference of some 2% – 3% in Table III. This must be because of the measuring accuracy of the temperature. The temperature of the rotor was measured with a sensors glued in the slots where the magnets were assembled. The sensors were not actually touching the magnets. It can be that the temperature of the magnets was a bit different from the temperature of the sensors. Another reason for the difference can be, that the different sensors were showing different temperature readings during the testing. The difference between the maximum and the minimum reading was around 5°C . The testing was started when the highest reading reached the decided temperature, because it was assumed that the magnets

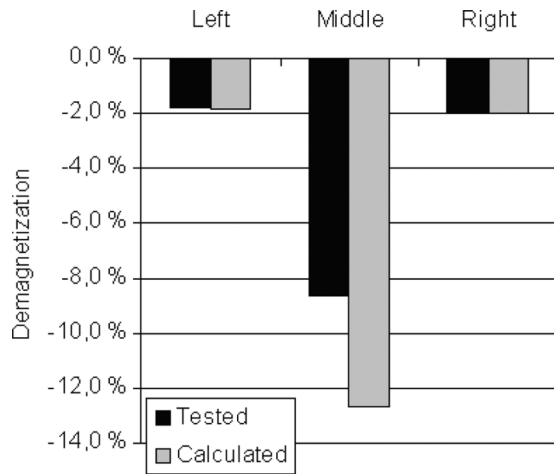


Fig. 9. A measured demagnetization (drop of magnetic polarization) of the poles after the locked-rotor situation with 100 Hz, 165 A input compared to the calculated demagnetization. This machine had a mixed-grade construction with grade A on the side magnets and grade B on the middle magnet. The mass of the middle magnet is twice the mass of the side magnet.

TABLE III
RESULTS OF THE LOCKED-ROTOR DEMAGNETIZATION TESTING

Rotor Construction (Magnet grades on magnet: Side – Middle – Side)	Measured Test Conditions (Current, Min Temp ... Max Temp)	Calculated demagnetization (drop of EMF) (in Temp)	Calculated demagnetization (drop of magnetic polarization) (in Temp)	Demagnetization after the test (drop of magnetic polarization)
Single-Grade Rotor (A – A – A)	165 A, 174°C... 179°C	-6.3 % (180°C)	-6.2 % (180°C)	-3.4 %
Mixed-Grade Rotor (A – B – A)	160 A, 168°C... 173°C	-7.8 % (175°C)	-7.3 % (175°C)	-5.3 %

might be a bit hotter than the sensors. It was assumed, that the eddy currents in the magnets are causing heating in the rotor.

When comparing the demagnetization on a magnet-by-magnet basis (Figs. 8 and 9), it can be seen that the calculations and the test results show quite a similar behavior. In Fig. 8, the demagnetization of the middle magnet is less than the demagnetization of the side magnet both in the calculations and according to the testing. The situation in Fig. 9 is opposite both in the test and calculations.

The calculation results presented in Fig. 8 show higher demagnetization than the test results. The reason for this must be that the temperature in the rotor was not as high in the test. The average measured rotor temperature in the test was 175 °C, while in the calculations the temperature of the magnet material was 180 °C. Also, a slight error in the intrinsic coercivity in calculations can have direct consequences in the results. The calculation results in Fig. 9 are closer to the test results. The average measured temperature in the test was 172 °C, while the temperature of the magnets used in the calculations was 175 °C.

This testing shows that the demagnetization calculation method used can predict the demagnetization of the magnet

TABLE IV
COMPARISON OF DIFFERENT ROTOR CONSTRUCTIONS

Rotor Construction (Magnet grades on magnet: Side – Middle – Side)	Temperature, at which -5% demagnetization happens in a locked-rotor situation with 165 A input current (Fig. 3)	Calculated EMF in 20°C	Cost Difference
Single-Grade Rotor (A – A – A)	179°C	391.3 V	0 EUR
Mixed-Grade Rotor (A – B – A)	173°C	394.7 V	-0.89 EUR
Single-Grade Rotor (B – B – B)	170 °C	398.1 V	-1.78 EUR

material in a permanent magnet machine with a reasonable accuracy (Figs. 8 and 9). It was noticed that the temperature is the most important factor affecting the accuracy of the calculations (Fig. 3). The temperature deviation of the real rotor cannot be modeled in the 2-D model used, which will cause inaccuracy when modeling rotors with very high temperature deviation.

The mixed-grade construction tested was developed from a tested single-grade construction by changing the middle magnet from magnet grade A to magnet grade B, while keeping the side magnets made of grade A. The assumed benefits were an improved EMF, lower magnet cost and only a slightly inferior demagnetization resistance. The EMF of the single-grade construction was 391.3 V, while the EMF of the mixed-grade construction was 394.7 V, showing some 1% increase.

The price of Nd and Dy were at the level of 87 EUR/kg and 13 EUR/kg respectively at late 2008 [16]. By changing from grade A to grade B, 1% of Dy can be replaced by Nd in a magnet chemistry causing a potential saving of 0.74 EUR/kg for the magnet cost. This machine has 2.4 kg of magnet material. In the mixed-grade construction, a half of this magnet material was replaced by grade B, making the cost saving in euros quite small. In larger machines, however, the cost saving can be more significant.

According to Figs. 6 and 8, the side-magnets are first demagnetized in a locked-rotor situation in the single-grade construction. Thus, it can be expected that the middle magnet does not need as much intrinsic coercivity as the side magnets. To improve the construction, the mixed-grade construction was created by replacing the middle magnet made of grade A with a magnet made of grade B. Now, according to Fig. 9, the middle magnet demagnetizes first, suggesting that the change of intrinsic coercivity in the middle magnet was too large.

When comparing the calculated demagnetization resistances according to Fig. 3, it can be seen that the demagnetization resistance of the mixed-grade construction is slightly inferior to the demagnetization resistance of the single-grade construction based on grade A, as expected. The same applies to the three-phase short circuit situation. At 170 °C the demagnetizations of the single-grade construction and the mixed-grade construction are -0.5% and -2.2%, respectively. However, because the EMF of these constructions is different, the difference in remaining EMF after the demagnetization is only 0.8% at

170 °C. In Fig. 3 it can be seen that at 165 °C the demagnetization resistance of the studied constructions is at the similar level.

The two single-grade and one mixed-grade constructions are compared in Table IV.

VI. CONCLUSION

A dovetail machine using a mixed-grade magnet construction was introduced. The demagnetization in an overheated locked-rotor situation was calculated using a demagnetization model introduced in earlier papers. The demagnetization in the same situation was also tested with a real motor, and the results were compared.

It was shown by comparing calculations and a real situation testing, that the demagnetization model used can predict the demagnetization of the permanent magnets in an electric machine with a reasonable accuracy, taking also into account the temperature dependence of the magnetic properties.

The potential improvement of the properties of a mixed-grade construction was discussed. It was shown that by using a mixed-grade construction, the flux of the machine can be increased while the demagnetization resistance becomes only slightly inferior. Simultaneously, the cost of the magnet material is slightly decreased.

ACKNOWLEDGMENT

This work was supported by Finnish Cultural Foundation, Research Foundation of Helsinki University of Technology, Ulla Tuomisen Säätiö, and High Technology Foundation of Satakunta. The authors would like to thank Neorem Magnets Oy for the magnet samples and ABB Oy Machines for testing facilities.

REFERENCES

- [1] J. Kolehmainen and J. Ikäheimo, "Motors with buried magnets for medium-speed applications," *IEEE Trans. Energy Convers.*, vol. 23, no. 1, pp. 86–91, Mar. 2008.
- [2] J. Kolehmainen, "Rotor for a Permanent-Magnet Electrical Machine," WO Patent 2008025873 (A1), Mar. 6, 2008.
- [3] J. Kolehmainen, "Machine with a rotor structure supported only by buried magnets," presented at the Int. Symp. Electromagnetic Fields, Prague, Sep. 2007.
- [4] J. Kolehmainen, "Dovetail permanent magnet rotor solutions with different pole numbers," in *Proc. 2008 Int. Conf. Electrical Machines*, Paper ID 939.
- [5] S. Ruoho and A. Arkkio, "Mixed-grade pole design for permanent magnet synchronous machines," presented at the ACEMP'07 and ELECTROMOTION'07 Joint Meeting, Bodrum, Turkey, Sep. 10–12, 2007.
- [6] J. Farooq, S. Srairi, A. Djerdir, and A. Miraoui, "Use of permeance network method in the demagnetization phenomenon modeling in a permanent magnet motor," *IEEE Trans. Magn.*, vol. 42, no. 4, pp. 1295–1298, Apr. 2006.
- [7] G.-H. Kang, J. Hur, H.-G. Sung, and J.-P. Hong, "Optimal design of spoke type BLDC motor considering irreversible demagnetization of permanent magnet," in *Sixth Int. Conf. Electrical Machines and Systems, ICEMS 2003*, vol. 1, pp. 234–237.
- [8] G.-H. Kang, J. Hur, H. Nam, J.-P. Hong, and G.-T. Kin, "Analysis of irreversible magnet demagnetization in line-start motors based on the finite-element method," *IEEE Trans. Magn.*, vol. 39, no. 3, pp. 1488–1491, May 2003.

- [9] B.-K. Lee, G.-H. Kang, J. Hur, and D.-W. You, "Design of spoke type BLDC motors with high power density for traction applications," in *IEEE Industry Applications Conf.*, 2004, vol. 2, pp. 1068–074.
- [10] K.-C. Kim, S.-B. Lim, D.-H. Koo, and J. Lee, "The shape design of permanent magnet for permanent magnet synchronous motor considering partial demagnetization," *IEEE Trans. Magn.*, vol. 42, no. 10, pp. 3485–3487, Oct. 2006.
- [11] M. Rosu, J. Saitz, and A. Arkkio, "Hysteresis model for finite-element analysis of permanent-magnet demagnetization in a large synchronous motor under a fault condition," *IEEE Trans. Magn.*, vol. 41, no. 6, pp. 2118–2123, Jun. 2005.
- [12] J. H. Lee and J. P. Hong, "Permanent magnet demagnetization characteristic analysis of a variable flux memory motor using coupled Preisach modeling and FEM," *IEEE Trans. Magn.*, vol. 44, no. 6, pp. 1550–1553, Jun. 2008.
- [13] J. Wang, W. Wang, K. Atallah, and D. Howe, "Demagnetization assessment for three-phase tubular brushless permanent-magnet machines," *IEEE Trans. Magn.*, vol. 44, no. 9, pp. 2195–2203, Sep. 2008.
- [14] S. Ruoho, E. Dlala, and A. Arkkio, "Comparison of demagnetization models for finite-element analysis of permanent magnet synchronous machines," *IEEE Trans. Magn.*, vol. 43, no. 11, pp. 3964–3968, Nov. 2007.
- [15] S. Ruoho and A. Arkkio, "Partial demagnetization of permanent magnets in electrical machines caused by an inclined field," *IEEE Trans. Magn.*, vol. 44, no. 7, pp. 1773–1778, Jul. 2008.
- [16] Chinese Rare-Earth Prices [Online]. Available: www.asianmetal.com Dec. 2008
- [17] Front Page [Online]. Available: www.magnetweb.com Mar. 2008
- [18] A. Arkkio, "Analysis of Induction Motors Based on the Numerical Solution of the Magnetic Field and Circuit Equations," Ph.D. thesis, Acta Polytechnica Scandinavica, no. 59, Helsinki, Finland, 1987.
- [19] M. Katter, "Angular dependence of the demagnetization stability of sintered Nd-Fe-B magnets," *IEEE Trans. Magn.*, vol. 41, no. 10, pp. 3853–3855, Oct. 2005.

Sami Ruoho was born in Pori, Finland, in 1973. He received the M.Sc. degree in applied physics from the University of Turku, Finland, in 1997. He is now pursuing the Ph.D. degree at the Laboratory of Electromechanics, Helsinki University of Technology (TKK), Finland. His subject is the modeling of demagnetization of permanent magnets in permanent-magnet machines.

Since 2002, he has been working for Neorem Magnets Oy, a company manufacturing sintered Nd-Fe-B-magnets in Finland as a Research Engineer and as an Application Engineer. During his studies he still works part time for Neorem Magnets Oy (www.neorem.fi).

Jere Kolehmainen was born in Kuopio, Finland, in 1972. He received the M.Sc. and Ph.D. degrees in theoretical physics from University of Jyväskylä, Jyväskylä, Finland, in 1996 and 2000, respectively.

Currently, he is working at ABB Oy, Motors, Vaasa, Finland. His research interests include synchronous and induction AC machines and electromagnetic modeling.

Jouni Ikäheimo was born in Seinäjoki, Finland, in 1968. He received the M.Sc. and Ph.D. degrees in theoretical physics from Helsinki University of Technology, Espoo, Finland, in 1992 and 1996, respectively.

He is currently an R&D manager with ABB Oy, Motors, Vaasa, Finland.

Antero Arkkio was born in Vehkalahti, Finland, in 1955. He received his M.Sc. (Tech.) and D.Sc. (Tech.) degrees from Helsinki University of Technology, Finland, in 1980 and 1988, respectively.

He has been a Professor of electrical engineering (Electromechanics) at Helsinki University of Technology (TKK) since 2001. Before his appointment as a Professor, he was a Senior Research Scientist and Laboratory Manager at TKK. He has worked with various research projects dealing with modeling, design, and measurement of electrical machines.